Available online at www.sciencedirect.com

ScienceDirect

Advances in Climate Change Research xxx (xxxx) xxx

www.keaipublishing.com/en/journals/accr/

Variability and trends of near-surface wind speed over the Tibetan Plateau: The role played by the westerly and Asian monsoon

Gang-Feng ZHANG[a,b,c], Cesar AZORIN-MOLINA[d], Deliang CHEN[e], Tim R. MCVICAR[f,g], Jose A. GUIJARRO[h], Kai-Qiang DENG[i], Lorenzo MINOLA[d,e,j], Jaeyeon LEE[k,l,m], Seok-Woo SON[k], Heng MA[a,b,c], Pei-Jun SHI[a,b,c,*]

[a] *State Key Laboratory of Earth Surface Processes and Resource Ecology, Beijing Normal University, Beijing 100875, China*
[b] *Engineering Center of Desertification and Blown-Sand Control of Ministry of Education, Faculty of Geographical Science, Beijing Normal University, Beijing 100875, China*
[c] *Key Laboratory of Environmental Change and Natural Disaster of Ministry of Education, Beijing Normal University, Beijing 100875, China*
[d] *Centro de Investigaciones Sobre Desertificación, Consejo Superior de Investigaciones Cientficas (CIDE, CSIC-UV-Generalitat Valenciana), Climate, Atmosphere and Ocean Laboratory (Climatoc-Lab), Moncada 46113, Spain*
[e] *Regional Climate Group, Department of Earth Sciences, University of Gothenburg, Gothenburg 40530, Sweden*
[f] *CSIRO Environment, Canberra, ACT 2600, Australia*
[g] *Australian Research Council Centre of Excellence for Climate Extremes, Canberra, ACT 2600, Australia*
[h] *State Meteorological Agency, Balearic Islands Office, Palma de Mallorca 07015, Spain*
[i] *School of Atmospheric Sciences, Sun Yat-sen University, Zhuhai 519082, China*
[j] *Interuniversity Department of Regional and Urban Studies and Planning (DIST), Politecnico and University of Turin, Turin 10125, Italy*
[k] *School of Earth and Environmental Sciences, Seoul National University, Seoul 08826, South Korea*
[l] *Atmospheric and Oceanic Sciences Program, Princeton University, Princeton NJ 08544, USA*
[m] *Geophysical Fluid Dynamics Laboratory, NOAA, Princeton NJ 08544, USA*

Received 12 August 2023; revised 7 November 2023; accepted 9 April 2024

Abstract

Near-surface wind speed exerts profound impacts on many environmental issues, while the long-term (≥60 years) trend and multidecadal variability in the wind speed and its underlying causes in global high-elevation and mountainous areas (*e.g.*, Tibetan Plateau) remain largely unknown. Here, by examining homogenized wind speed data from 104 meteorological stations over the Tibetan Plateau for 1961−2020 and ERA5 reanalysis datasets, we investigated the variability and long-term trend in the near-surface wind speed and revealed the role played by the westerly and Asian monsoon. The results show that the homogenized annual wind speed displays a decreasing trend (−0.091 m s^{-1} per decade, $p < 0.05$), with the strongest in spring (−0.131 m s^{-1} per decade, $p < 0.05$), and the weakest in autumn (−0.071 m s^{-1} per decade, $p < 0.05$). There is a distinct multidecadal variability of wind speed, which manifested in an prominent increase in 1961−1970, a sustained decrease in 1970−2002, and a consistent increase in 2002−2020. The observed decadal variations are likely linked to large-scale atmospheric circulation, and the correlation analysis unveiled a more important role of westerly and East Asian winter monsoon in modulating near-surface wind changes over the Tibetan Plateau. The potential physical processes associated with westerly and Asian monsoon changes are in concordance with wind speed change, in terms of overall weakened horizontal air flow (*i.e.*, geostrophic wind speed), declined vertical thermal and dynamic momentum transfer (*i.e.*, atmospheric stratification thermal instability and vertical wind shear), and varied Tibetan Plateau vortices. This indicates that to

* Corresponding author. State Key Laboratory of Earth Surface Processes and Resource Ecology, Beijing Normal University, Beijing 100875, China.
E-mail address: spj@bnu.edu.cn (SHI P.-J.).
Peer review under responsibility of National Climate Centre (China Meteorological Administration).

https://doi.org/10.1016/j.accre.2024.04.007
1674-9278/© 2024 The Authors. Publishing services by Elsevier B.V. on behalf of KeAi Communications Co. Ltd. This is an open access article under the CC BY-NC-ND license (http://creativecommons.org/licenses/by-nc-nd/4.0/).

Please cite this article as: ZHANG, G.-F et al., Variability and trends of near-surface wind speed over the Tibetan Plateau: The role played by the westerly and Asian monsoon, Advances in Climate Change Research, https://doi.org/10.1016/j.accre.2024.04.007

varying degrees these processes may have contributed to the changes in near-surface wind speed over the Tibetan Plateau. This study has implications for wind power production and soil wind erosion prevention in the Tibetan Plateau.

Keywords: Tibetan Plateau; Wind speed; Decadal change; Atmospheric circulation; Physical processes

1. Introduction

A secular decline in terrestrial winds since the 1960s was found, termed 'stilling' (Roderick et al., 2007). This negative trend is reported for many mid-latitude low-elevation regions such as Australia (McVicar et al., 2008), the USA (Pryor et al., 2009), Spain and Portugal (Azorin-Molina et al., 2014), eastern China (Li et al., 2022) and numerous other locations globally (McVicar et al., 2012). However, the global stilling ceased around 2013 and may have reversed slightly afterward (Zeng et al., 2019; Azorin-Molina et al., 2021). Regional wind studies reported a cessation of the 'stilling' or even reversal in land near-surface wind speeds for the Iberian Peninsula (Utrabo-Carazo et al., 2022), Saudi Arabia (Azorin-Molina et al., 2018a), Sweden (Minola et al., 2022), and northern China (Zhang et al., 2021). Due to the limited observations and poor quality of wind speed data, wind speed variability in global high-elevation and mountainous areas, such as the Tibetan Plateau (TP), has only received minor attention (McVicar et al., 2010; You et al., 2014; Wu et al., 2018). For example, previous study has found that wind speed at high elevation is declining more quickly than at low elevations in both China and Switzerland (McVicar et al., 2010), while opposite wind speed trends were observed below and above the trade-wind inversion layer in the Canary Islands (Azorin-Molina et al., 2018b). Several previous studies reported an overall decline in near-surface wind speed over the TP using anemometer observations for various periods (Lin et al., 2013; Guo et al., 2017; Ding et al., 2021), and noted a distinct variability in wind speed trends (Table A1). They did not employ quality control and homogenization methods to the raw wind speed series, making the quantitative estimate questionable.

Since more than 60% of the TP is arid or semiarid, near-surface wind is one of the most important factors shaping local landform and geographical environment (Dong et al., 2017), and their changes have prominent environmental implications. The near-surface wind speed strongly affects evapotranspiration in the TP (Song et al., 2017), and hence regulates its hydrological cycle (Yang et al., 2014). Strong wind (*i.e.*, >5 m s^{-1}), along with sparse vegetation cover, also poses a serious wind erosion threat to the barren soils across the TP (Jiang et al., 2021), triggering frequent dust storms (Kang et al., 2016). Due to abundant wind power resources, wind electricity production in the TP plays a key role in renewable energy development (Sherman et al., 2017). Moreover, near-surface wind speed change also exerts impacts on many other environmental and ecological processes in the TP, such as wildfire activity (Wang et al., 2023) and pollen emission (Lü et al., 2020).

The near-surface wind speed variability is driven by many factors and physical processes, such as atmospheric circulation changes (Azorin-Molina et al., 2018a; Wu et al., 2018), vegetation growth (Vautard et al., 2010), rapid urbanization (Zhang et al., 2022), effects of local air pollution (Jacobson and Kaufman, 2006), and instrumentation issues (Azorin-Molina et al., 2023). The TP winds are primarily modulated by interactions between the Asian monsoon and mid-latitude westerlies (Yao et al., 2012; Nie et al., 2017). For example, near-surface wind speed in the southwestern TP is mainly determined by the Indian summer monsoon (Ding et al., 2021), while mid-latitude westerlies are the primary driver of wind speed over the western TP (Wang et al., 2016). Considering the dynamics of wind speeds in high-elevation or mountainous areas (*e.g.*, TP), accurate attribution of their causes becomes more challenging as atmospheric circulation strongly interacts with land surface and complex terrain (Xue et al., 2017; Yao et al., 2019; Zha et al., 2022).

The TP has experienced faster warming during the last decades compared to the surrounding low-elevation areas and the global mean (Yao et al., 2019; You et al., 2021), which has further altered the interaction between the Asian monsoon and mid-latitude westerlies (Yao et al., 2019). Due to the complex topographic environment (Yao et al., 2012), there are strong valley winds in the high mountainous area (Yang et al., 2018), and frequently occurring synoptic circulations (*e.g.*, the TP vortex, Wu et al., 2022) also strongly affect wind speed over the TP. Previous research demonstrated elevation-dependent change in climate changes over the TP (*e.g.*, You et al., 2020) and confirmed that dynamics of wind speed were strongly determined by local terrain and geographical settings. These effects have enhanced the uncertainty and the difficulty in accurately assessing potential causes of TP wind speed dynamics. In a warming climate, there is still a lack of understanding regarding the potential causes of wind speed variability over the TP. It remains unclear whether westerly winds and the Asian monsoon have played the same role in influencing changes in TP wind speeds and the underlying physical processes driving these changes.

Given the aforementioned, this study aims to investigate long-term (*i.e.*, 60 years) trends and multidecadal variability in homogenized annual and seasonal mean near-surface wind speeds, and reveal the potential causes. This study enhances the understanding of stilling and recent reversal of near-surface wind speeds, and has implications for near-surface wind speed changes related wind erosion and wind power production in the TP.

Please cite this article as: ZHANG, G.-F et al., Variability and trends of near-surface wind speed over the Tibetan Plateau: The role played by the westerly and Asian monsoon, Advances in Climate Change Research, https://doi.org/10.1016/j.accre.2024.04.007

2. Data and methods

2.1. Observed data

Wind speed observations (at 10-m height) at four-time steps (from 2000 to 2000 UTC the next day) with 6-h intervals from the China Meteorological Administration (CMA) are used to calculate daily mean series, consisting of 104 stations covering the TP (Fig. 1), with the highest TP station (*i.e.*, Bangge) at 4701 m a.s.l. As many CMA stations started to record wind speed in 1960, the analysis covered from 1961 to 2020, to avoid the low station density of the earlier years.

Daily wind speed observations were aggregated into monthly values, allowing a maximum of five missing days in each month. Further, stations were eliminated when too much missing data occurred (*i.e.*, 8 months in total in 1961−2020). Station resettlement, anemometer type replace (Wan et al., 2010), and anemometer aging (Azorin-Molina et al., 2018c) can induce artificial bias in raw wind speed series. As successfully applied in previous works (*e.g.*, Azorin-Molina et al., 2018a; Zhang et al., 2021), the Climatol package (Guijarro, 2018; http://www.climatol.eu/; last accessed on 1 January 2024) was used to implement quality control, homogenization process, and missing data infilling on the 104 raw near-surface wind speed series, using the ERAS reanalysis wind speed as reference data. More details of the homogenization can be found in Azorin-Molina et al. (2018a) and Zhang et al. (2020). The homogenized wind speed series has eliminated the impacts of non-climatic factors in raw wind speed (Fig. A1), and has been utilized in the analysis presented in the results section.

2.2. Reanalysis data

Reanalysis data including monthly wind at surface, 500 and 450 hPa, geopotential height at 500 hPa, and atmospheric pressure at the surface, air temperature at 500, 300, and 200 hPa, and hourly 500 hPa relative vorticity were obtained from the ERA5 dataset (https://cds.climate.copernicus.eu/cdsapp#!/search?type=dataset&text=ERA5; 0.25 × 0.25°, Dee et al., 2011) from 1961 to 2020.

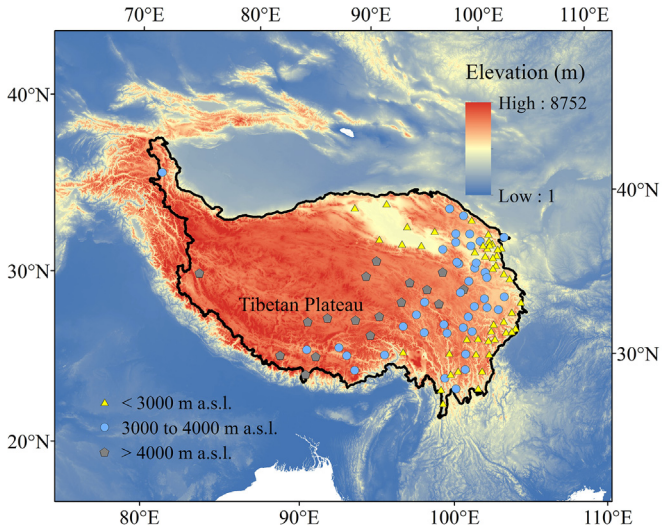

Fig. 1. Terrain map showing the distribution of the 104 homogenized meteorological stations over the Tibetan Plateau.

2.3. Asian monsoon and westerlies modes

To uncover the influences of interactions between the Asian monsoon and westerlies on wind speed changes over the TP, relationships between wind speed and Asian monsoon and westerlies modes were investigated. The indices representing these modes were listed in Table A2, and including the East Asian summer monsoon index (EASMI; Li and Zeng, 2002; Li et al., 2010), the Indian summer monsoon index (ISMI; Wang et al., 2001), East Asian winter monsoon index (EAWMI; Wang and He, 2012), and the Westerly Index (WI; Vicente-Serrano et al., 2016). Additionally, a well-established Tibetan Plateau Index (TPI; You et al., 2014) that indicated the activity of anticyclone over the TP was used. The TPI was significantly related to wind speed over the TP (You et al., 2014). All of the indices in 1961−2020 were derived from the National Climate Centre of China Meteorological Administration (http://cmdp.ncc-cma.net/cn/index.htm).

The physical processes of Asian monsoon and westerlies modes regulating wind speed were firstly represented by the regional horizontal pressure-gradient force at 500 hPa (Zhang et al., 2020). Further, changes in the regional atmospheric vertical momentum transport were expressed as, atmospheric thermal stratification instability (the A index, Zhang et al., 2014), and vertical wind shear between 500 hPa and 450 hPa (Zhang et al., 2020).

Mesoscale to synoptic-scale weather system were identified by the TP vortexes (TPV; Hodges, 1994, 1999). Briefly, TPVs are detected with local maxima in the 6-h 500-hPa relative vorticity field, subject to T40-100 spatial filtering. Only vorticity maxima greater than 0.2 s^{-1}, which originated on the TP above the 3000-m altitude and persisted for at least 1 d, are accounted for. Following Curio et al. (2019), a geopotential minimum filter is additionally applied. Specifically, TPV tracks that have 500-hPa geopotential height minimum within a search radius of 2.5° × 2.5° around the TPV center at least for one time step are considered. See Curio et al. (2019) for full details.

2.4. Statistics analyses

Wind speed trends (in m s^{-1} per decade) was computed by Sen's slope method (Atta-ur-Rahman and Dawood, 2017; Collaud Coen et al., 2020), and the multidecadal variability of wind speed was illustrated by an 11-year Gaussian low-pass filter. Mann−Kendall's tau-b non-parametric correlation coefficient was applied to determine the statistical significance of trends (Zhang et al., 2020). The turning point of wind speed variability indicate the end of previous subperiod and the start of new subperiod, and it was included in both subperiod. Two *p*-level thresholds ($p < 0.05$ and $p > 0.05$) were used. Besides, the relationship between atmospheric circulation modes and wind speed variability was exhibited by the Pearson correlation coefficient (*r*). The multiple linear regression was used to quantify

Please cite this article as: ZHANG, G.-F et al., Variability and trends of near-surface wind speed over the Tibetan Plateau: The role played by the westerly and Asian monsoon, Advances in Climate Change Research, https://doi.org/10.1016/j.accre.2024.04.007

the explained variances of atmospheric circulation indices to wind speed (Shi et al., 2019). Note that in the regression analysis of winter wind speed, summer monsoon indices are not included. Similarly, winter monsoon indices are not considered in the regression of summer wind speed. The atmospheric circulation indies modeled wind speed was based on piecewise linear regression, and calculated by the function between atmospheric circulation indices and wind speed (Zeng et al., 2019).

3. Results

3.1. Multidecadal variability and trends of near-surface wind speed

The annual mean wind speed exhibits a significant ($p < 0.05$) decreasing trend of -0.091 m s^{-1} per decade, with seasonal series also having an overall significant decreasing trend for all seasons (Fig. 2 and Table 1). Specifically, spring experienced the strongest decreasing trend (-0.137 m s^{-1} per decade), and autumn shows the weakest negative trend. The 11-year Gaussian low pass filter uncovers three phases (sub-periods) for the annual mean wind speed, a prominent increasing phase from 1961 to 1970 (0.188 m s^{-1} per decade, $p > 0.05$), a significant decreasing phase from 1970 to 2002 (-0.269 m s^{-1} per decade, $p < 0.05$), and an increasing or reversal phase after 2002 (0.073 m s^{-1} per decade, $p < 0.05$). These three phases can also be detected in the seasonally averaged wind speed series (Fig. 2). However, wind speed from ERA5 shows a relatively stable interannual variability for 1961−2020 (Fig. A2).

The significant negative trend ($p < 0.05$) recorded in 87.5% of the stations for annual wind speed (Table A3). Most stations (>90.0%) are related to a slowdown in wind speed for all seasons, although this occurs less frequently for winter (93.3%) and summer (95.2%) than for autumn (96.2%) and spring (100%). Noted that an upward wind speed trend occurred in some stations, which may be induced by local environmental changes, such as glacier breezes (Conway et al., 2021). In 1961−1970, annual (75.0%, Table A3) and seasonal wind speed (68.3%−79.8%, Table A3) increased in most regions of the TP, while decreased wind speeds were detected at northeastern, southern and northwestern margins of the TP (Fig. A3). During 1970−2002, all the stations had decreasing trends (ranging between -0.1 and -0.5 m s^{-1} per decade) in annual and all seasons (Fig. A4, Fig. 2). During 2002−2020, an interesting pattern occurred, that is, most of the stations located in the northern TP showed a decreasing trend, while increasing trend was found in most of the stations located in the southern TP (Fig. A5). When looking at wind speed trends from ERA5 (Fig. A6), a similar pattern with declined winds was found in the northern TP, while the southern TP showed an increasing trend.

3.2. Relationship with westerly and Asian monsoon modes

Table 2 reports the correlation between annual near-surface wind speed and atmospheric circulation indices response to the westerly and Asian monsoon from 1961 to 2020. The correlation coefficients of EASMI/ISMI and the TP wind speed were weak, while both indices were significantly correlated with wind speeds at some stations located in southeastern TP ($p < 0.05$, Fig. A7). EAWMI had a significant positive correlation ($r = 0.37$, $p < 0.05$) with wind speed over the TP, especially for those stations at southeastern and east-western TP (Fig. A7). WI and TPI had a significant negative correlation with the TP wind speed, and this is true for most stations in the TP (Fig. A7). Annual EAWMI significantly

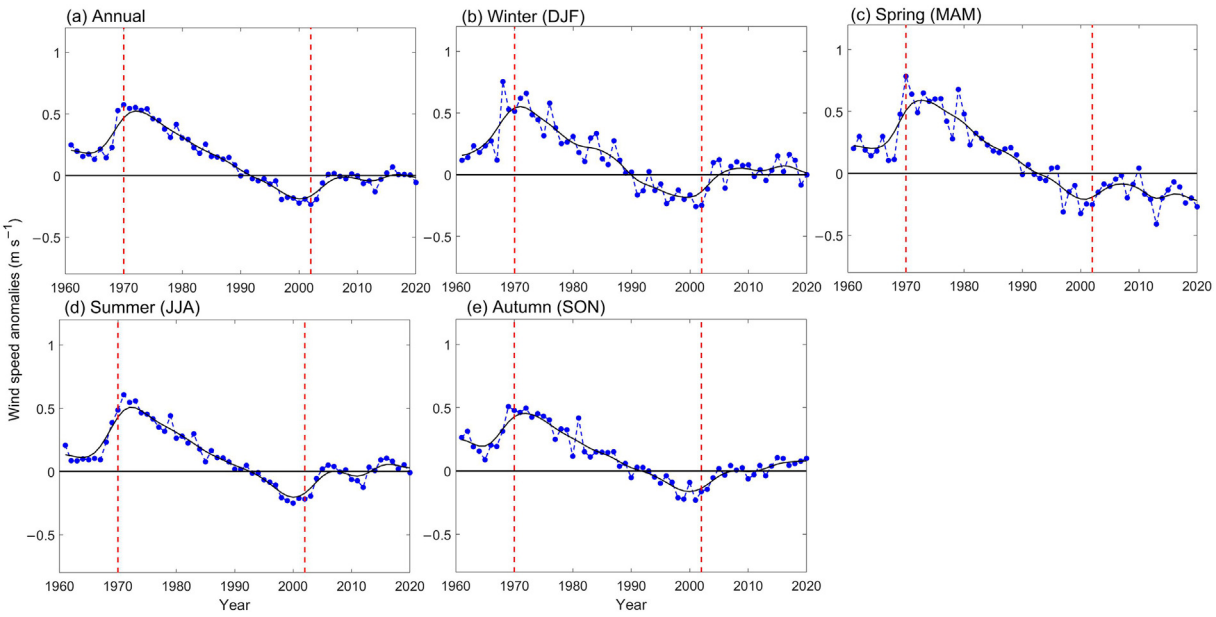

Fig. 2. Annual and seasonal mean near-surface wind speed anomalies (relative to 1981−2010) for the Tibetan Plateau as a whole for 1961−2020 (The black solid lines indicate the 11-year Gaussian low-pass filter. The two red dashed vertical lines (years 1970 and 2002) indicate the division of the three sub-periods).

Please cite this article as: ZHANG, G.-F et al., Variability and trends of near-surface wind speed over the Tibetan Plateau: The role played by the westerly and Asian monsoon, Advances in Climate Change Research, https://doi.org/10.1016/j.accre.2024.04.007

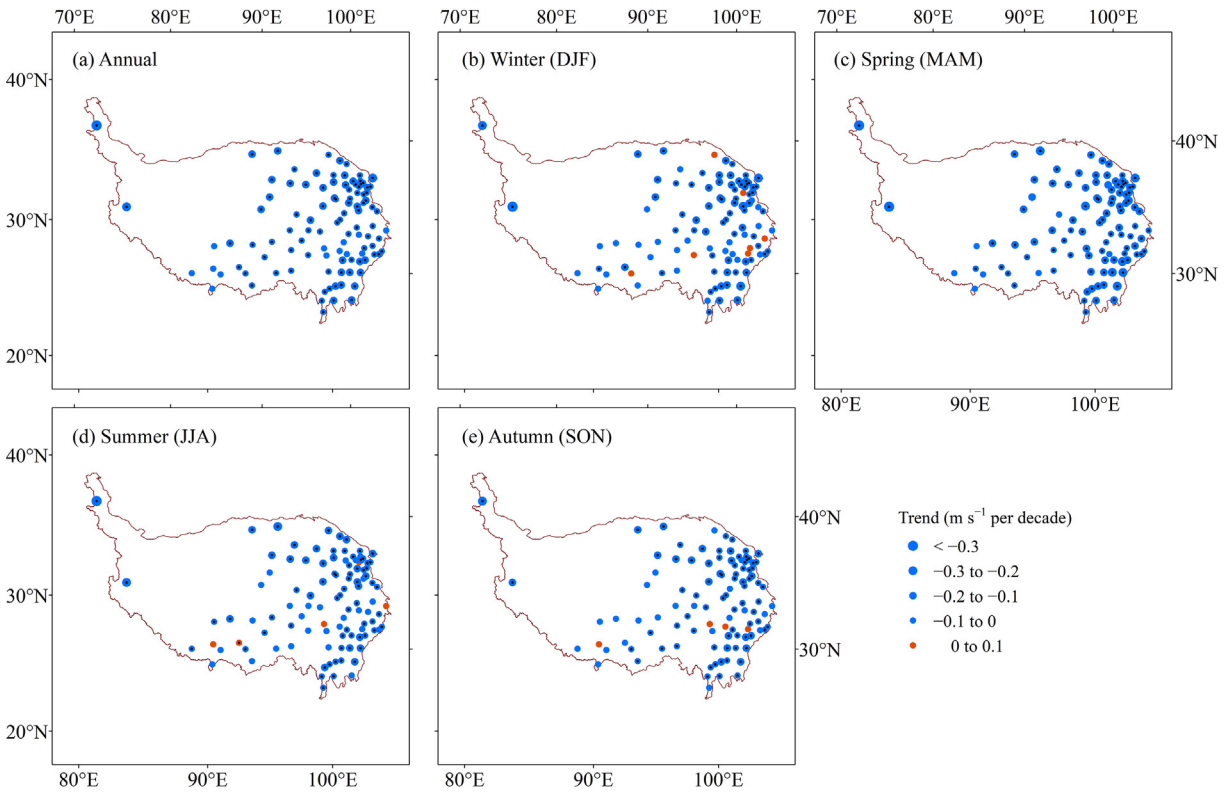

Fig. 3. Spatial distribution of the sign and magnitude of annual and seasonal observed near-surface wind speed trends over the Tibetan Plateau for 1961−2020 (A small black dot in a circle indicates a significant trend at $p < 0.05$).

decreased (−0.26 per decade, $p < 0.05$) during 1961−2020, and TPI significantly increased (28.7 per decade, $p < 0.05$) (Fig. A8), which can partly explain the overall declined wind speed in the TP (Yang et al., 2021; You et al., 2014, Fig. 2a).

By using piecewise linear regression, Table 3 summarizes the variance of near-surface wind speed changes explained by westerly and Asian monsoon modes that exhibit significant correlations with the TP wind speed during three sub-periods in the TP. How the near-surface wind speeds were reproduced based on the significantly correlated westerly and Asian monsoon indices is shown in Fig. 4. Annually, westerly and Asian monsoon modes contributed the highest variance (52.4%) of wind speed changes over the TP in 1961−1970, followed by 1970−2002 (49.8%) and 2002−2020 (42.4%). The reconstructed wind speeds were overall consistent with observed wind speed for the three sub-periods (Fig. 4), especially for 1960−1970 ($r = 0.72$, $p < 0.05$, Table A4), which indicates that wind speed across the study region was largely modulated by westerly and Asian monsoon changes. Seasonally, the westerly and Asian monsoon modes explained the highest wind speed variance during 1960−1970 in spring (67.0%) and summer (56.7%). In contrast, autumn (68.1%) and summer (56.6%) wind speeds were largely regulated by westerly and Asian monsoon changes during 1970−2002. In 2002−2020, westerly and Asian monsoon modes contributed less than 50% of near-surface wind speed variances in all seasons (13.2%−47.8%).

3.3. Potential physical processes associated with westerly and Asian monsoon circulation change

Given the close relation between westerly and Asian monsoon circulation and near-surface wind speed across the TP, the interacted physical processes behind westerly and

Table 1
Trends in annual and seasonal mean near-surface wind speed (m s^{-1} per decade) for the TP as a whole from 1961 to 2020 and in the three sub-phases.

Season	1961−2020	1961−1970	1970−2002	2002−2020
Annual	**−0.091**	0.188	**−0.269**	**0.073**
Winter	**−0.084**	**0.466**	**−0.270**	0.102
Spring	**−0.131**	0.194	**−0.308**	−0.005
Summer	**−0.075**	**0.224**	**−0.264**	**0.125**
Autumn	**−0.071**	0.238	**−0.229**	**0.122**

Note: Statistically significant values ($p < 0.05$) are bolded.

Table 2
Correlation coefficient of EASMI, ISMI, EAWMI, WI and TPI with observed annual and seasonal near-surface wind speed series for the TP as a whole for 1961−2020.

Season	EASMI	ISMI	ESWM	WI	TPI
Annual	0.13	0.15	**0.37**	**−0.28**	**−0.53**
Winter	–	–	**0.35**	**−0.31**	−0.01
Spring	0.02	**0.26**	**0.44**	**−0.39**	**−0.38**
Summer	0.09	0.17	–	−0.24	**−0.41**
Autumn	0.21	0.05	**0.34**	−0.04	**−0.59**

Note: Statistically significant values at $p < 0.05$ are bolded.

Please cite this article as: ZHANG, G.-F et al., Variability and trends of near-surface wind speed over the Tibetan Plateau: The role played by the westerly and Asian monsoon, Advances in Climate Change Research, https://doi.org/10.1016/j.accre.2024.04.007

Table 3
Total contributions (%) of the westerly and Asian monsoon modes to near-surface wind speed variance during three sub-periods for the TP.

Season	1961−1970	1970−2002	2002−2020
Annual	52.4	49.8	42.4
Winter	43.0	38.8	29.9
Spring	67.0	34.5	13.2
Summer	56.7	56.6	29.5
Autumn	37.1	68.1	47.8

Asian monsoon circulation influencing wind speed were explored. Fig. 5 exhibits the spatial distribution of annual and seasonal geostrophic wind speed trends over the TP and surroundings from 1961 to 2020, Annually, geostrophic wind speed widely declined over the TP, especially in the northeastern part (−0.4 to −0.8 m s^{-1} per decade, $p < 0.05$), corresponding to the spatial pattern of observed wind speed trends (Fig. 3a). This indicates that the overall declined regional atmospheric circulation over the TP may have contributed to the weakened wind speed. Seasonally, negative trends of geostrophic wind speed were found in most parts of the study region in all seasons, especially for winter and spring (−1.2 to 0 m s^{-1}). When compared with the seasonal wind speed changes, it is seen that the geostrophic wind speed trend is consistent with near-surface wind speed trends (Fig. 3b−d). Although, there are some exceptions in summer and autumn, as the opposite trends between geostrophic wind speed and near-surface wind speed over the southeastern TP. These patterns imply that westerly and Asian monsoon induced horizontal air flow decline is partly responsible for the decrease in wind speed over the Tibetan Plateau.

Moreover, the changes in the vertical thermal and dynamic transport of atmospheric momentum from 1961 to 2020 are represented by trends of the A index (Fig. 6) and vertical wind shear (Fig. 7). Most of the plateau experienced negative trends of the annual A index, with significant trends ($p < 0.05$) in southeastern and northeastern TP. Meanwhile. vertical wind shear weakly declined over the TP ($p > 0.05$). Both patterns indicate that the weakened dynamic and thermal vertical momentum transport likely caused the slowdown of wind speed (Fig. 3a). Seasonally, both winter atmospheric thermal stratification instability and vertical wind shear declined over the most area of the TP. Those patterns demonstrate a weakened vertical thermal and dynamic transport of atmospheric momentum, which is in line with the declined wind speed during the study period. Furthermore, spring witnessed negative trends of the A index in most parts, with significant areas ($p < 0.05$) occurring in the northern TP. At the same time, vertical wind shear trends had negative trends (−0.1 to 0 m s^{-1} per decade) in the northern and southwestern TP. Those showed agreement with the wind speed trends pattern (Fig. 3c). For summer, few southern and eastern parts showed negative trends of the A index, while vertical wind shear declined in most of the study region. Lastly, the A index experienced widely negative trends in autumn, barring parts of the northern TP, where a weakened thermal vertical momentum transfer in the middle and low troposphere can be seen. The decreases in vertical momentum transfer, along with the overall decline in horizontal air flows represented by geostrophic wind changes, emphasizes the crucial role of westerly and Asian monsoon systems in weakening wind speed over the TP.

The annual and seasonal trends of the frequency of TPV are illustrated in Fig. A9. They are associated with mesoscale and synoptic-scale processes over the TP. The annual TPV frequency shows a weak negative trend ($p > 0.1$) for the whole study period, due to the cancellation between positive trends in southern TP and negative trends in part of northern TP. This

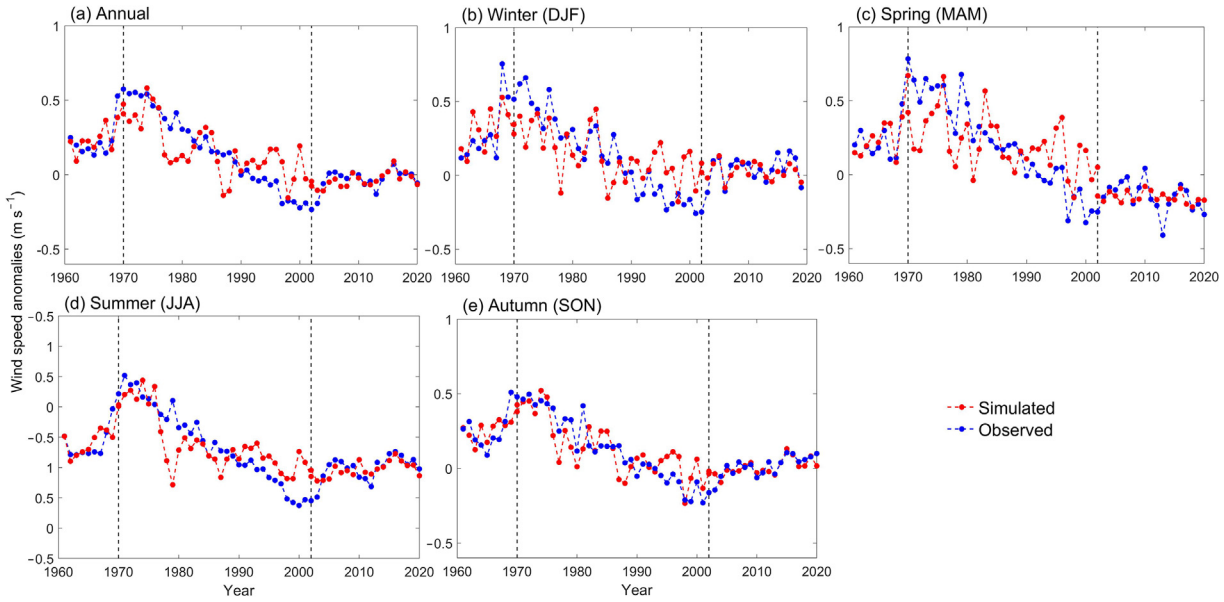

Fig. 4. Variability of observed and piecewise linear regression modeled annual and seasonal near-surface wind speed over the Tibetan Plateau from 1961 to 2020 (The two dashed vertical lines indicate 1970 and 2002, respectively).

Please cite this article as: ZHANG, G.-F et al., Variability and trends of near-surface wind speed over the Tibetan Plateau: The role played by the westerly and Asian monsoon, Advances in Climate Change Research, https://doi.org/10.1016/j.accre.2024.04.007

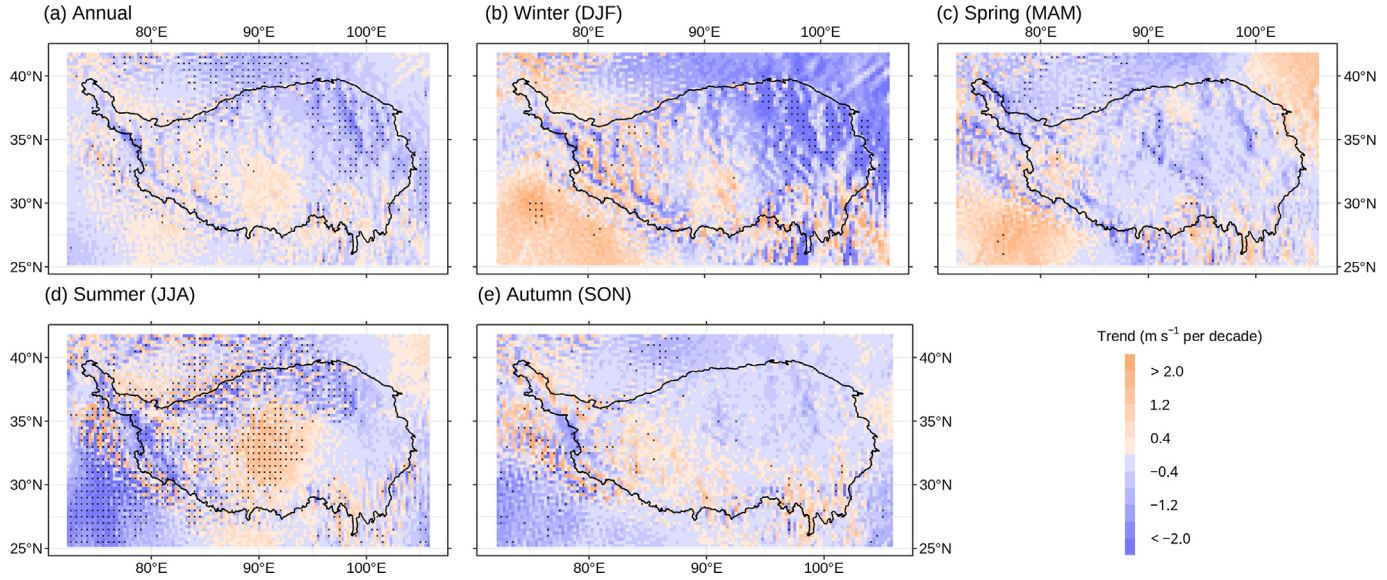

Fig. 5. Spatial distribution of annual and seasonal geostrophic wind speed trends at 500 hPa across the Tibetan Plateau and surrounds for 1961−2020 (*$p < 0.05$).

partly concords with the overall declined annual wind speed. This result indicates that TPV frequency change may be responsible for the wind speed change in the northern TP. When it comes to the seasons, an increased TPV frequency is found in winter ($p > 0.05$) and autumn ($p > 0.05$). Locally TPV frequency change ranges from 0 to +0.8 per decade in winter and from 0 to +1.6 per decade in autumn. This result is contrary to the declined winter and autumn wind speed for most of the TP. However, TPV frequency has decreased in spring ($p > 0.05$) and summer ($p > 0.1$), with stronger negative trends in northern TP in spring and southern TP in summer. This is consistent with the weakened summer and autumn wind speed and indicates that summer and autumn wind speed changes might be related to declined TPV frequency.

4. Discussion

Fig. 8 demonstrates a schematic summary for the variability and possible causes of near-surface wind speed changes over the TP. Our current work provided timely evidence that the wind stilling and reversal phenomenon can be seen in the TP, the world's highest plateau, as homogenized wind speed over

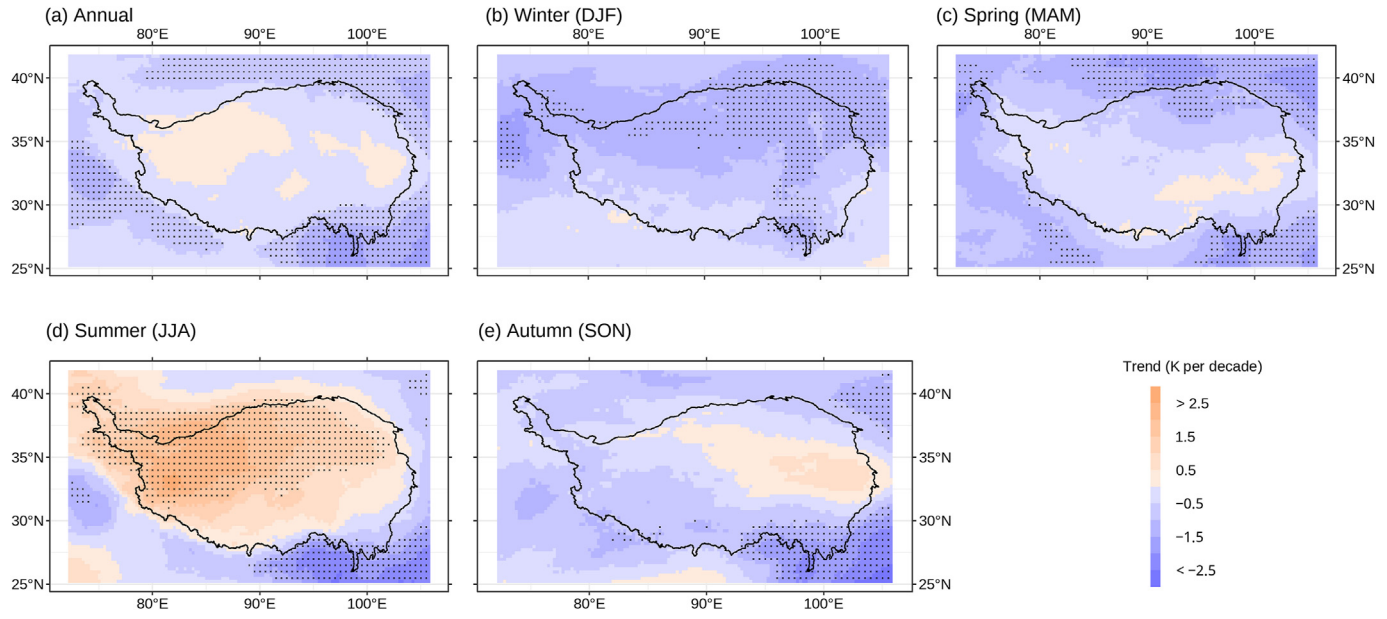

Fig. 6. Annual and seasonal spatial distribution of the sign and magnitude and associated statistical significance of the atmospheric thermal stratification instability (the A index, K) between 200 hPa and 500 hPa trends across the Tibetan Plateau and surrounds for 1961−2020 (*$p < 0.05$).

Please cite this article as: ZHANG, G.-F et al., Variability and trends of near-surface wind speed over the Tibetan Plateau: The role played by the westerly and Asian monsoon, Advances in Climate Change Research, https://doi.org/10.1016/j.accre.2024.04.007

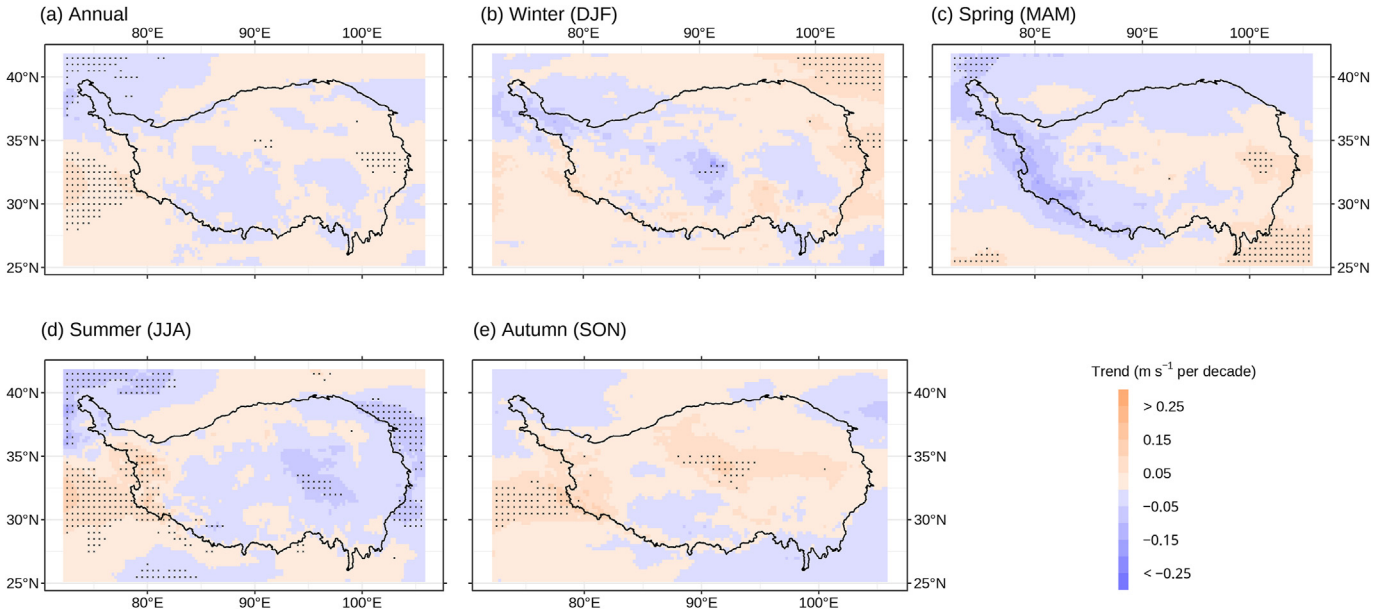

Fig. 7. Spatial distribution of trends in the annual and seasonal vertical wind shear between 450 hPa and 500 hPa across the Tibetan Plateau and surrounds for 1961−2020 (*$p < 0.05$).

this region significantly declined during 1970−2002 and increased after 2002. The homogenized data have high quality by infilling the missing data, removing and fixing possible breakpoints caused by non-climatic factors, while the trends of raw wind speed are close to trends from homogenized data (Fig. A1; Table A5). In fact, with homogenizing a series where break-points are present, trends would more related to climatic changes rather than artificial factors (Azorin-Molina et al., 2019; Minola et al., 2022). As booming wind energy resources exploitation is rapidly becoming an integral part of many nation's energy strategies (Gao et al., 2018; Pryor and Barthelmie, 2021; Sherman et al., 2020), a general reversal of winds will benefit the wind energy production in the TP and may facilitate it to become the first carbon neutral region in China. However, enhanced wind speed can trigger more frequently occurred wind erosion (Zhang et al., 2017), which may further cause serious land degradation and should be taken into account when designing and implementing environmental and ecological protection programs.

Limited to the observed wind speed data for a long-term period (*e.g.*, ≥60 years), the multidecadal variability of wind speed is still not fully addressed. For example, existing studies showed that wind stilling can last for around 30−40 years, and ceased from the 1990s to the 2010s (Zeng et al., 2019; Azorin-Molina et al., 2021). Although many recent works reported the reversal of wind speed, to date, this new phenomenon has only been observed for 10−30 years (Azorin-Molina et al., 2018c; Zha et al., 2021; Minola et al., 2022). An interesting question now is 'How long the increased wind speed tendency will continue'? Due to the long-term dataset (*i.e.*, 60 years) utilized

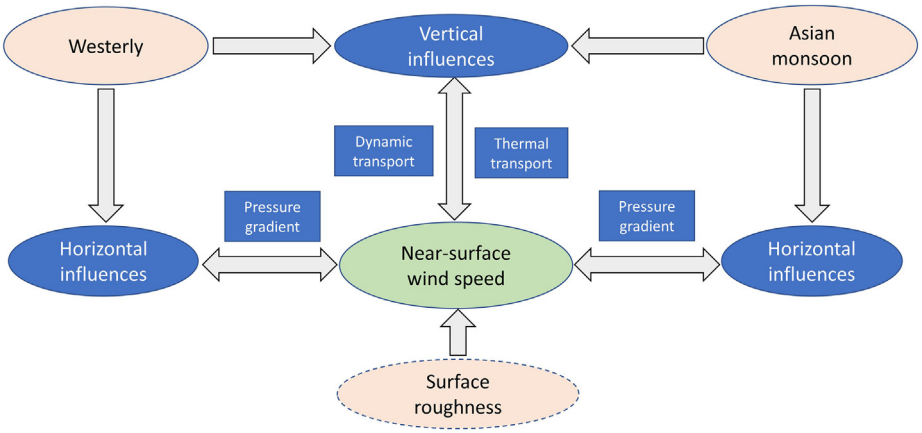

Fig. 8. Schematic frameworks of variability and possible causes of near-surface wind speed changes over the TP (The green color represents the factors driving changes in near-surface wind speed, while the blue color signifies the physical processes associated with atmospheric circulation modes that impact near-surface wind speed. The dashed line around 'Surface roughness' indicates this was not considered herein).

Please cite this article as: ZHANG, G.-F et al., Variability and trends of near-surface wind speed over the Tibetan Plateau: The role played by the westerly and Asian monsoon, Advances in Climate Change Research, https://doi.org/10.1016/j.accre.2024.04.007

in this study, we can see that the total period of wind stilling in the TP is 33 years (Fig. 2). Based on the record of lake sediments in northern China, a periodic change in wind speed was found while the total cycle of wind speed (increased wind speed and decreased wind speed) varied from ~60 to 70 years (Xu et al., 2019). While this finding is in line with our speculation, we strongly advocate that more direct records of long-term (*i.e.*, century or more) wind speed observations, and proxies of wind speed (*e.g.*, Fang et al., 2022), be curated and analyzed for as many locations as possible.

We compared the spatial distribution of wind speed trends at different sub-periods. Most of the stations in the northern Tibetan Plateau continue to display a decrease in wind speed during the period of wind reversal, even though most of the stations in the southern TP have significant positive trends, thus wind reversal trends should be interpreted cautiously. Previous studies documented different start dates of wind reversal in different continents (Zeng et al., 2019; Azorin-Molina et al., 2021), while this study suggests that wind recovery is not spatially synchronous in a region with complex terrain. It should be noted that the northwestern TP, which is characterized by complex topography, lacks long-term wind speed observations (Fig. 1). As a result, there are significant uncertainties regarding the variability of wind speeds in these high-elevation mountainous regions.

Our analyses suggest that TP wind speed dynamics are largely regulated by westerly, while the role played by Asian monsoon is less evident, except for the stations in the low-elevation southeastern TP. This might be related to the intensity attenuation of these summer monsoon circulations with the increased distance between the origins and the mountainous mainland TP (Kathayat et al., 2017; Son et al., 2019). Note that the EAWMI shows a higher correlation with spring TP winds than winter; this is likely due to the key role played by the westerlies on winds in spring. The EAWM represents the intensity of the Siberian high-pressure system, which primarily regulates westerlies affecting winds in the TP (Yang et al., 2021). That westerly and Asian monsoon modes together explain 42.7%−82.8% variance of the seasonal mean wind speed changes in the TP confirms the key role of westerly and Asian monsoon on modulating wind speed variability (Wu et al., 2018; Zeng et al., 2019). Note that the explained variance of the wind speed changes in the last sub-period is relatively low. This suggests that other factors, such as changes in local circulation (*e.g.*, glacier breeze), may have played a more significant role in regulating wind speed changes during that time. Furthermore, we revealed that deceased regional pressure gradient, and widely weakened vertical thermal and dynamic transport of atmospheric momentum, contributed to the overall declined wind speed. The pattern of TPV trends is partly consistent with the near-surface wind speed, while the spatial and temporal scale of TPV is relatively small compared to the large-scale changes of surface winds. This indicates that the TPV can also be affected by the changes in large-scale wind speed. If we compare the changes of those physical processes in the latter two sub-periods (*i.e.*, 1970−2002 and 2002−2020), it was seen that vertical transport of atmospheric momentum also reversed (Figs. A10 and A11), when wind stilling turned to wind recovery. This indicates that the recent recovery in the TP can be partly attributed to physical processes associated with atmospheric circulation vertical changes.

Although a large part of interannual TP wind speed variability can be explained by the westerly and Asian monsoon changes (Table 3), there are other factors such as vegetation recovery (Vautard et al., 2010; Wever, 2012; Zhang et al., 2019) and urbanization (Chen et al., 2020), which may have played a role and are not considered in this study. For example, a secular increased NDVI (Normalized Difference Vegetation Index, a proxy of vegetation cover) was detected from 1982 to 2002 in the TP (Zhang et al., 2013; Pang et al., 2017), which indicates that the increased roughness caused by greening may have contributed to the declined wind speed during this period (Vautard et al., 2010). However, vegetation has had continuous growth in the TP since 2002 (Li et al., 2018), which is contrary to the wind reversal since 2002. This means large-scale atmospheric circulation change is most likely a more dominant factor to recent wind reversal detected in the TP, rather than vegetation change. Nevertheless, the consistently increased vegetation over recent decades is likely to be postponing or attenuating the observed reversal of near-surface wind speeds (Zhang et al., 2021). It is worthwhile to quantify the contribution of vegetation growth to near-surface wind speed changes by analyzing sensitivity experiments in regional climate models (Wang et al., 2020; Zhang et al., 2022), This will enhance our understanding of the drivers of near-surface wind speed for the TP.

5. Conclusion

(1) Overall, annual mean near-surface wind speed over the TP significantly declined from 1961 to 2020. Seasonal wind speed trends displayed a similar pattern, with the highest negative trend for spring and the lowest for autumn.
(2) The annual mean TP wind speed experienced a pronounced periodic change on the multi-decadal scale. Specifically, it abruptly increased from 1961 to 1970, then significantly declined from 1970 to 2002, before a consistent recovering since 2002.
(3) The prevailing westerly and Eastern Asian winter monsoon play a more important role than the East Asian summer monsoon and the Indian summer monsoon in modulating the near-surface TP wind speed variability. The westerly and Asian monsoon circulations together explain 42.4%−52.4% of the variance of annual wind speed and 13.2%−68.1% of the variance of seasonal wind speed in three sub-periods.
(4) Changes in four interacting physical processes were suggested to explain how the westerly and Asian monsoon circulation influence the detected wind speed changes. These include declined regional pressure gradient force; both weakened vertical thermal momentum transfer and vertical dynamic momentum transfer, and varied TPVs frequency.

Please cite this article as: ZHANG, G.-F et al., Variability and trends of near-surface wind speed over the Tibetan Plateau: The role played by the westerly and Asian monsoon, Advances in Climate Change Research, https://doi.org/10.1016/j.accre.2024.04.007

Declaration of competing interest

The authors declare no conflict of interest.

Acknowledgments

The authors wish to acknowledge Prof. Yihui Ding, the Editors and the two anonymous reviewers for their detailed and helpful comments to the original manuscript. This research was supported by the National Natural Science Foundation of China (42101027), the Second Tibetan Plateau Scientific Expedition and Research Program (STEP, 2019QZKK0606), the Fundamental Research Funds for the Central Universities of China (2022NTST18), and Opening Foundation of Engineering Center of Desertification and Blown-Sand Control of Ministry of Education at Beijing Normal University (2023-B-2). This work was also supported by the IBER-STILLING project, funded by the Spanish Ministry of Science. L.M. was founded by an International Postdoc grant from the Swedish Research Council (2021-00444). SWS was supported by 'Development of Advanced Science and Technology for Marine Environmental Impact Assessment' of Korea Institute of Marine Science & Technology Promotion (KIMST) funded by the Ministry of Oceans and Fisheries of South Korea (20210427).

Appendix A. Supplementary data

Supplementary data to this article can be found online at https://doi.org/10.1016/j.accre.2024.04.007.

References

Atta-ur-Rahman, Dawood, M., 2017. Spatio-statistical analysis of temperature fluctuation using Mann−Kendall and Sen's slope approach. Clim. Dynam. 48, 783−797. https://doi.org/10.1007/s00382-016-3110-y.

Azorin-Molina, C., Asin, J., McVicar, T.R., et al., 2018a. Evaluating anemometer drift: a statistical approach to correct biases in wind speed measurement. Atmos. Res. 203, 175−188. https://doi.org/10.1016/j.atmosres.2017.12.010.

Azorin-Molina, C., Menendez, M., McVicar, T.R., et al., 2018b. Wind speed variability over the Canary Islands, 1948−2014: focusing on trend differences at the land−ocean interface and below−above the trade-wind inversion layer. Clim. Dynam. 50, 4061−4081. https://doi.org/10.1007/s00382-017-3861-0.

Azorin-Molina, C., Dunn, R.J.H., Ricciardulli, L., et al., 2021. Land and ocean surface winds. Bull. Am. Meteorol. Soc. 102, S73−S77. https://doi.org/10.1175/2021BAMSStateoftheClimate.1.

Azorin-Molina, C., Guijarro, J.A., McVicar, T.R., et al., 2019. An approach to homogenize daily peak wind gusts: an application to the Australian series. Int. J. Climatol. 39, 2260−2277. https://doi.org/10.1002/joc.5949.

Azorin-Molina, C., Pirooz, A.A.S., Bedoya-Valestt, S., et al., 2023. Biases in wind speed measurements due to anemometer changes. Atmos. Res. 289, 106771. https://doi.org/10.1016/j.atmosres.2023.106771.

Azorin-Molina, C., Rehman, S., Guijarro, J.A., et al., 2018c. Recent trends in wind speed across Saudi Arabia, 1978−2013: a break in the stilling. Int. J. Climatol. 38, e966−e984. https://doi.org/10.1002/joc.5423.

Azorin-Molina, C., Vicente-Serrano, S.M., Mcvicar, T.R., et al., 2014. Homogenization and assessment of observed near-surface wind speed trends over Spain and Portugal, 1961−2011. J. Clim. 27, 3692−3712. https://doi.org/10.1175/JCLI-D-13-00652.1.

Chen, X., Jeong, S., Park, H., et al., 2020. Urbanization has stronger impacts than regional climate change on wind stilling: a lesson from South Korea. Environ. Res. Lett. 15. https://doi.org/10.1088/1748-9326/ab7e51.

Collaud Coen, M., Andrews, E., Bigi, A., et al., 2020. Effects of the pre-whitening method, the time granularity, and the time segmentation on the Mann−Kendall trend detection and the associated Sen's slope. Atmos. Meas. Tech. 13, 6945−6964. https://doi.org/10.5194/amt-13-6945-2020.

Conway, J.P., Helgason, W.D., Pomeroy, J.W., et al., 2021. Icefield breezes: mesoscale diurnal circulation in the atmospheric boundary layer over an outlet of the columbia icefield, Canadian rockies. J. Geophys. Res. Atmos. 126, 1−17. https://doi.org/10.1029/2020JD034225.

Curio, J., Schiemann, R., Hodges, K.I., et al., 2019. Climatology of Tibetan Plateau vortices in reanalysis data and a high-resolution global climate model. J. Clim. 32, 1933−1950. https://doi.org/10.1175/JCLI-D-18-0021.1.

Dee, D.P., Uppala, S.M., Simmons, A.J., et al., 2011. The ERA-Interim reanalysis: configuration and performance of the data assimilation system. Q. J. R. Meteorol. Soc. 137, 553−597. https://doi.org/10.1002/qj.828.

Ding, J., Cuo, L., Zhang, Y., et al., 2021. Varied spatiotemporal changes in wind speed over the Tibetan Plateau and its surroundings in the past decades. Int. J. Climatol. 1−21. https://doi.org/10.1002/joc.7162.

Dong, Z., Hu, G., Qian, G., et al., 2017. High-altitude aeolian research on the Tibetan Plateau. Rev. Geophys. 55, 864−901. https://doi.org/10.1002/2017RG000585.

Fang, K., Bai, M., Azorin-Molina, C., et al., 2022. Wind speed reconstruction from a tree-ring difference index in northeastern Inner Mongolia. Dendrochronologia 72, 125938. https://doi.org/10.1016/j.dendro.2022.125938.

Gao, M., Ding, Y., Song, S., et al., 2018. Secular decrease of wind power potential in India associated with warming in the Indian Ocean. Sci. Adv. 4. https://doi.org/10.1126/sciadv.aat5256.

Guijarro, J.A., 2018. Homogenization of climatic series with Climatol. State Meteorol. Agency (AEMET), Balear Islands Office, Spain.

Guo, X., Wang, L., Tian, L., et al., 2017. Elevation-dependent reductions in wind speed over and around the Tibetan Plateau. Int. J. Climatol. 37, 1117−1126. https://doi.org/10.1002/joc.4727.

Hodges, K.I., 1999. Adaptive constraints for feature tracking. Mon. Weather Rev. 127, 1362−1373. https://doi.org/10.1175/1520-0493(1999)127<1362:acfft>2.0.co;2.

Hodges, K.I., 1994. A general method for tracking analysis and its application to meteorological data. Mon. Weather Rev. 122, 2573−2586. https://doi.org/10.1175/1520-0493(1994)122<2573:AGMFTA>2.0.CO;2.

Jacobson, M.Z., Kaufman, Y.J., 2006. Wind reduction by aerosol particles. Geophys. Res. Lett. 33, 1−6. https://doi.org/10.1029/2006GL027838.

Jiang, Y., Gao, Y., He, C., et al., 2021. Spatiotemporal distribution and variation of wind erosion over the Tibetan Plateau based on a coupled land−surface wind-erosion model. Aeolian Res 50, 100699. https://doi.org/10.1016/j.aeolia.2021.100699.

Kang, L., Huang, J., Chen, S., et al., 2016. Long-term trends of dust events over Tibetan Plateau during 1961−2010. Atmos. Environ. 125, 188−198. https://doi.org/10.1016/j.atmosenv.2015.10.085.

Kathayat, G., Cheng, H., Sinha, A., et al., 2017. The Indian monsoon variability and civilization changes in the Indian subcontinent. Sci. Adv. 3, 1−9. https://doi.org/10.1126/sciadv.1701296.

Li, J., Wu, Z., Jiang, Z., et al., 2010. Can global warming strengthen the East Asian summer monsoon? J. Clim. 23, 6696−6705. https://doi.org/10.1175/2010JCLI3434.1.

Li, J., Zeng, Q., 2002. A unified monsoon index. Geophys. Res. Lett. 29, 1−4. https://doi.org/10.1029/2001GL013874.

Li, L., Zhang, Y., Liu, L., et al., 2018. Spatiotemporal patterns of vegetation greenness change and associated climatic and anthropogenic drivers on the Tibetan Plateau during 2000−2015. Remote Sens 10, 1−16. https://doi.org/10.3390/rs10101525.

Li, X., Li, Q.P., Ding, Y.H., et al., 2022. Near-surface wind speed changes in eastern China during 1970−2019 winter and its possible causes. Adv. Clim. Change Res. 13, 228−239. https://doi.org/10.1016/j.accre.2022.01.003.

Lin, C., Yang, K., Qin, J., et al., 2013. Observed coherent trends of surface and upper-air wind speed over China since 1960. J. Clim. 26, 2891−2903. https://doi.org/10.1175/JCLI-D-12-00093.1.

Please cite this article as: ZHANG, G.-F et al., Variability and trends of near-surface wind speed over the Tibetan Plateau: The role played by the westerly and Asian monsoon, Advances in Climate Change Research, https://doi.org/10.1016/j.accre.2024.04.007

Lü, X., Paudayal, K.N., Uhl, D., et al., 2020. Phenology and climatic regime inferred from airborne pollen on the northern slope of the Qomolangma (everest) region. J. Geophys. Res. Atmos. 125, e2020JD033405. https://doi.org/10.1029/2020JD033405.

McVicar, T.R., Van Niel, T.G., Li, L.T., et al., 2008. Wind speed climatology and trends for Australia, 1975−2006: capturing the stilling phenomenon and comparison with near-surface reanalysis output. Geophys. Res. Lett. 35, 1−6. https://doi.org/10.1029/2008GL035627.

McVicar, T.R., Van Niel, T.G., Roderick, M.L., et al., 2010. Observational evidence from two mountainous regions that near-surface wind speeds are declining more rapidly at higher elevations than lower elevations: 1960−2006. Geophys. Res. Lett. 37, 1−6. https://doi.org/10.1029/2009GL042255.

McVicar, T.R., Roderick, M.L., Donohue, R.J., et al., 2012. Global review and synthesis of trends in observed terrestrial near-surface wind speeds: implications for evaporation. J. Hydrol. 416−417, 182−205. https://doi.org/10.1016/j.jhydrol.2011.10.024.

Minola, L., Reese, H., Lai, H.W., et al., 2022. Wind stilling-reversal across Sweden: the impact of land-use and large-scale atmospheric circulation changes. Int. J. Climatol. 42, 1049−1071. https://doi.org/10.1002/joc.7289.

Nie, J., Garzione, C., Su, Q., et al., 2017. Dominant 100,000-year precipitation cyclicity in a late Miocene lake from northeast Tibet. Sci. Adv. 3, 1−10. https://doi.org/10.1126/sciadv.1600762.

Pang, G., Wang, X., Yang, M., 2017. Using the NDVI to identify variations in, and responses of, vegetation to climate change on the Tibetan Plateau from 1982 to 2012. Quat. Int. 444, 87−96. https://doi.org/10.1016/j.quaint.2016.08.038.

Pryor, S.C., Barthelmie, R.J., 2021. A global assessment of extreme wind speeds for wind energy applications. Nat. Energy 6, 268−276. https://doi.org/10.1038/s41560-020-00773-7.

Pryor, S.C., Barthelmie, R.J., Young, D.T., et al., 2009. Wind speed trends over the contiguous United States. J. Geophys. Res. Atmos. 114, D14105. https://doi.org/10.1029/2008JD011416.

Roderick, M.L., Rotstayn, L.D., Farquhar, G.D., et al., 2007. On the attribution of changing pan evaporation. Geophys. Res. Lett. 34, 1−6. https://doi.org/10.1029/2007GL031166.

Sherman, P., Chen, X., McElroy, M.B., 2017. Wind-generated electricity in China: decreasing potential, inter-annual variability and association with changing climate. Sci. Rep. 7, 1−10. https://doi.org/10.1038/s41598-017-16073-2.

Sherman, P., Chen, X., McElroy, M., 2020. Offshore wind: An opportunity for cost-competitive decarbonization of China's energy economy. Sci. Adv. 6, 1−9. https://doi.org/10.1126/sciadv.aax9571.

Shi, P., Zhang, G., Kong, F., et al., 2019. Variability of winter haze over the Beijing−Tianjin−Hebei region tied to wind speed in the lower troposphere and particulate sources. Atmos. Res. 215, 1−11. https://doi.org/10.1016/j.atmosres.2018.08.013.

Son, J.H., Seo, K.H., Wang, B., 2019. Dynamical control of the Tibetan Plateau on the East Asian summer monsoon. Geophys. Res. Lett. 46, 7672−7679. https://doi.org/10.1029/2019GL083104.

Song, L., Zhuang, Q., Yin, Y., et al., 2017. Spatio-temporal dynamics of evapotranspiration on the Tibetan Plateau from 2000 to 2010. Environ. Res. Lett. 12. https://doi.org/10.1088/1748-9326/aa527d.

Utrabo-Carazo, E., Azorin-Molina, C., Serrano, E., et al., 2022. Wind stilling ceased in the Iberian Peninsula since the 2000s. Atmos. Res. 272, 106153. https://doi.org/10.1016/j.atmosres.2022.106153.

Vautard, R., Cattiaux, J., Yiou, P., et al., 2010. Northern Hemisphere atmospheric stilling partly attributed to an increase in surface roughness. Nat. Geosci. 3, 756−761. https://doi.org/10.1038/ngeo979.

Vicente-Serrano, S.M., García-Herrera, R., Barriopedro, D., et al., 2016. The Westerly Index as complementary indicator of the North Atlantic oscillation in explaining drought variability across Europe. Clim. Dynam. 47, 845−863. https://doi.org/10.1007/s00382-015-2875-8.

Wan, H., Wang, X.L., Swail, V.R., 2010. Homogenization and trend analysis of Canadian near-surface wind speeds. J. Clim. 23, 1209−1225. https://doi.org/10.1175/2009JCLI3200.1.

Wang, B., Wu, R., Lau, K.M., 2001. Interannual variability of the Asian summer monsoon: contrasts between the Indian and the western North Pacific−East Asian monsoons. J. Clim. 14, 4073−4090. https://doi.org/10.1175/1520-0442(2001)014<4073:IVOTAS>2.0.CO;2.

Wang, H., He, S., 2012. Weakening relationship between East Asian winter monsoon and ENSO after mid-1970s. Chin. Sci. Bull. 57, 3535−3540. https://doi.org/10.1007/s11434-012-5285-x.

Wang, J., Feng, J., Yan, Z., et al., 2020. Urbanization impact on regional wind stilling: a modeling study in the Beijing−Tianjin−Hebei region of China. J. Geophys. Res. Atmos. 125, 1−17. https://doi.org/10.1029/2020JD033132.

Wang, X., Ren, J., Gong, P., et al., 2016. Spatial distribution of the persistent organic pollutants across the Tibetan Plateau and its linkage with the climate systems: a 5-year air monitoring study. Atmos. Chem. Phys. 16, 6901−6911. https://doi.org/10.5194/acp-16-6901-2016.

Wang, Z., Huang, R., Yao, Q., et al., 2023. Strong winds drive grassland fires in China. Environ. Res. Lett. 18. https://doi.org/10.1088/1748-9326/aca921.

Wever, N., 2012. Quantifying trends in surface roughness and the effect on surface wind speed observations. J. Geophys. Res. Atmos. 117, 1−14. https://doi.org/10.1029/2011JD017118.

Wu, G., Tang, Y., He, B., et al., 2022. Potential vorticity perspective of the genesis of a Tibetan Plateau vortex in June 2016. Clim. Dynam. https://doi.org/10.1007/s00382-021-06102-2.

Wu, J., Zha, J., Zhao, D., et al., 2018. Changes in terrestrial near-surface wind speed and their possible causes: an overview. Clim. Dynam. 51, 2039−2078. https://doi.org/10.1007/s00382-017-3997-y.

Xu, B., Gu, Z., Wang, L., et al., 2019. Global warming increases the incidence of haze days in China. J. Geophys. Res. Atmos. 6180−6190. https://doi.org/10.1029/2018JD030119.

Xue, Y., Ma, Y., Li, Q., 2017. Land−climate interaction over the Tibetan Plateau. Oxford Research Encyclopedia of Climate Science. https://doi.org/10.1093/acrefore/9780190228620.013.592.

Yang, K., Guyennon, N., Ouyang, L., et al., 2018. Impact of summer monsoon on the elevation-dependence of meteorological variables in the south of central Himalaya. Int. J. Climatol. 38, 1748−1759. https://doi.org/10.1002/joc.5293.

Yang, K., Wu, H., Qin, J., et al., 2014. Recent climate changes over the Tibetan Plateau and their impacts on energy and water cycle: a review. Global Planet Change 112, 79−91. https://doi.org/10.1016/j.gloplacha.2013.12.001.

Yang, L., Shi, Z., Sun, H., et al., 2021. Distinct effects of winter monsoon and westerly circulation on dust aerosol transport over East Asia. Theor. Appl. Climatol. 144, 1031−1042. https://doi.org/10.1007/s00704-021-03579-z.

Yao, T., Thompson, L.G., Mosbrugger, V., et al., 2012. Third Pole environment (TPE). Environ. Dev. 3, 52−64. https://doi.org/10.1016/j.envdev.2012.04.002.

Yao, T., Xue, Y., Chen, D., et al., 2019. Recent Third Pole's rapid warming accompanies cryospheric melt and water cycle intensification and interactions between monsoon and environment: multidisciplinary approach with observations, modeling, and analysis. Bull. Am. Meteorol. Soc. 100, 423−444. https://doi.org/10.1175/BAMS-D-17-0057.1.

You, Q., Cai, Z., Pepin, N., et al., 2021. Warming amplification over the Arctic Pole and Third Pole: trends, mechanisms and consequences. Earth Sci. Rev. 217, 103625. https://doi.org/10.1016/j.earscirev.2021.103625.

You, Q., Chen, D., Wu, F., et al., 2020. Elevation dependent warming over the Tibetan Plateau: patterns, mechanisms and perspectives. Earth Sci. Rev. 210, 103349. https://doi.org/10.1016/j.earscirev.2020.103349.

You, Q., Fraedrich, K., Min, J., et al., 2014. Observed surface wind speed in the Tibetan Plateau since 1980 and its physical causes. Int. J. Climatol. 34, 1873−1882. https://doi.org/10.1002/joc.3807.

Zeng, Z., Ziegler, A.D., Searchinger, T., et al., 2019. A reversal in global terrestrial stilling and its implications for wind energy production. Nat. Clim. Change 9, 979−985. https://doi.org/10.1038/s41558-019-0622-6.

Zha, J., Shen, C., Zhao, D., et al., 2021. Slowdown and reversal of terrestrial near-surface wind speed and its future changes over eastern China. Environ. Res. Lett. 16. https://doi.org/10.1088/1748-9326/abe2cd.

Zha, J.L., Shen, C., Wu, J., et al., 2022. Effects of Northern Hemisphere annular mode on terrestrial near-surface wind speed over eastern China from 1979 to 2017. Adv. Clim. Change Res. 13, 875−883. https://doi.org/10.1016/j.accre.2022.10.005.

Please cite this article as: ZHANG, G.-F et al., Variability and trends of near-surface wind speed over the Tibetan Plateau: The role played by the westerly and Asian monsoon, Advances in Climate Change Research, https://doi.org/10.1016/j.accre.2024.04.007

Zhang, G., Azorin-Molina, C., Chen, D., et al., 2020. Variability of daily maximum wind speed across China, 1975−2016: an examination of likely causes. J. Clim. 33, 2793−2816. https://doi.org/10.1175/JCLI-D-19-0603.1.

Zhang, G., Azorin-Molina, C., Chen, D., et al., 2021. Uneven warming likely contributed to declining near-surface wind speeds in northern China between 1961 and 2016. J. Geophys. Res. Atmos. 126, 1−24. https://doi.org/10.1029/2020JD033637.

Zhang, G., Azorin-molina, C., Wang, X., et al., 2022. Rapid urbanization induced daily maximum wind speed decline in metropolitan areas : a case study in the Yangtze River Delta (China). Urban Clim. 43, 101147. https://doi.org/10.1016/j.uclim.2022.101147.

Zhang, G., Zhang, Y., Dong, J., et al., 2013. Green-up dates in the Tibetan Plateau have continuously advanced from 1982 to 2011. Proc. Natl. Acad. Sci. U.S.A. 110, 4309−4314. https://doi.org/10.1073/pnas.1210423110.

Zhang, J.Q., Zhang, C.L., Chang, C.P., et al., 2017. Comparison of wind erosion based on measurements and SWEEP simulation: a case study in Kangbao county, Hebei province, China. Soil Tillage Res. 165, 169−180. https://doi.org/10.1016/j.still.2016.08.006.

Zhang, R.H., Li, Q., Zhang, R.N., 2014. Meteorological conditions for the persistent severe fog and haze event over eastern China in January 2013. Sci. China Earth Sci. 57, 26−35. https://doi.org/10.1007/s11430-013-4774-3.

Zhang, Z., Wang, K., Chen, D., et al., 2019. Increase in surface friction dominates the observed surface wind speed decline during 1973−2014 in the Northern Hemisphere lands. J. Clim. 32, 7421−7435. https://doi.org/10.1175/JCLI-D-18-0691.1.

Please cite this article as: ZHANG, G.-F et al., Variability and trends of near-surface wind speed over the Tibetan Plateau: The role played by the westerly and Asian monsoon, Advances in Climate Change Research, https://doi.org/10.1016/j.accre.2024.04.007